water

Article

The Runoff in the Upper Taohe River Basin and Its Responses to Climate Change

Lizhen Cheng [1,2], Guoning Wan [1], Meixue Yang [1,*], Xuejia Wang [3] and Yongshan Li [4]

[1] Yulong Snow Mountain Cryosphere and Sustainable Development Observation and Research Station/State Key Laboratory of Cryospheric Sciences, Northwest Institute of Eco-Environment and Resources, Chinese Academy of Sciences, Lanzhou 730000, China; lzcheng@lzb.ac.cn (L.C.); gnwan@lzb.ac.cn (G.W.)
[2] Bureau of Natural Resources and Planning of Yancheng, Yancheng 224000, China
[3] Key Laboratory of Western China's Environmental Systems (Ministry of Education), College of Earth and Environmental Sciences, Lanzhou University, Lanzhou 730000, China; xjwang@lzb.ac.cn
[4] School of Urban and Planning, Yancheng Teachers University, Yancheng 224000, China; liys@lzb.ac.cn
* Correspondence: mxyang@lzb.ac.cn

Abstract: Climate change has a significant impact on water resources. Forecasts and simulations of climate runoff processes are essential for assessing the impact of global climate change on runoff variations. This study focuses on the upper Taohe River Basin, which is an important watershed in the semi-arid regions of northwest China. To assess the runoff in the upper Taohe River Basin and the responses to climate change, the SWAT hydrological model was used to analyze future climate change scenarios and their effects on water resources. The results indicate that the minimum temperature would increase gradually in the 21st century and that the minimum temperature change would be more significant than the maximum temperature change, which indicates that minimum temperature changes would make an obvious contribution to future regional warming. Under RCP2.6, the average precipitation would decrease; at the same time, under RCP4.5 and RCP8.5, the average precipitation would increase. In the future, under different climate scenarios, the runoff will exhibit droughts and flood disasters. These research results provide scientific support for water resource utilization and management in the Taohe River Basin.

Keywords: climate change; runoff projection; hydrological models; Upper Taohe River basin

check for updates

Citation: Cheng, L.; Wan, G.; Yang, M.; Wang, X.; Li, Y. The Runoff in the Upper Taohe River Basin and Its Responses to Climate Change. *Water* **2022**, *14*, 2094. https://doi.org/10.3390/w14132094

Academic Editors: Nektarios N. Kourgialas, Ioannis Anastopoulos and Alexandros Stefanakis

Received: 3 June 2022
Accepted: 27 June 2022
Published: 30 June 2022

1. Introduction

Water resources have become one of the most important global resources and environmental problems in the 21st century and is also an essential aspect in international Earth science development [1–4]. Globally, rising temperatures due to continuous greenhouse gas emissions have exerted an irreversible impact on climate change, water resources, agriculture, health, energy, and natural systems. In the meantime, it has also added increased risk to the ecological environment as well as economic and social development in the future [5–11]. How to scientifically and quantitatively assess the impact of future climate change on regional hydrological processes has become a hot topic for meteorological and hydrological researchers [12,13]. Generally, the most scientific approach to predict climate change is based on physical assumptions that describe future global or regional climate change or climate change scenarios [14,15].

The Coupled Model Inter-comparison Project 5 (CMIP5) from the 5th Assessment Report (AR5) is the most successful of the General Circulation Models (GCMs)and includes four future scenarios: Representative Concentration Pathways (RCPs) 2.6, 4.5, 6.0, and 8.5. These scenarios are based on the expected differences in radiation, which have great impact on the future climate. In RCP2.6, scenarios can be found with radiative forcing as low as 3 W/m^2 in the year 2100. RCP4.5 and RCP6.0 assume the stabilization of radiative forcing. However, RCP8.5 assumes increased radiative forcing to 8.5 $W \cdot m^{-2}$ after 2100 [16].

Compared to global models, regional climate models (RCMs) with higher resolutions can not only describe the characteristics of large-scale circulation, but also accurately capture the characteristics of climate change at the regional scale [17–19]. Different scenarios generate different prediction trends for future climate change and have been widely used in global and regional climate change predictions.

Using hydrological models to simulate and predict the climate mechanism and hydrology processes is an important means to assess the impact of global climate change on runoff [20,21]. As a typical method of the distributed hydrological model, the SWAT (Soil and Water Assessment Tool) model has been successfully applied to the study of major watershed changes worldwide due to its mature and stable physical basis, and it has become an important tool for the study of water resource utilization and management [22,23]. The impact of future climate change on regional runoff has also become a hot issue of common concern to many domestic scholars in China [24–26]. For example, Wang et al. [27] found that the annual runoff gradually increases as the area of cultivated land converted to forest land increases in the middle and upper reaches of the Weihe River when using the SWAT model. Zubaida's study of the Urumqi River using the SWAT model found that the impact of climate change on runoff was more significant than the impact of land use changes [28]. Wang and Liu [29] used a statistical downscaling model to drive the SWAT hydrological model to predict the runoff of the Zamu River in northwest China. The results showed that the change rates of the runoff in the SRES A2 and B2 climate scenarios were −10.6~1.17% and −4~13%, respectively. Jin et al. [30] studied the future changes in water resources in the Haihe River Basin and found that the water resources will increase slightly from 2021 to 2050, especially in the north zone. In recent years, many researchers have used SWAT models driven by various climate models to study the runoff response of various typical regions, such as the source area of the Yellow River, Yangtze River Basin, and other major rivers.

The Taohe River, a large tributary of the upper reaches of the Yellow River, undertakes the task of water diversion for water scarcity areas in central Gansu Province through the Taohe River Diversion Project, which is in a key strategic position for the sustainable development of the regional social economy in Gansu Province. Under the background of climate warming, how will the water cycle and runoff change in the Tao River Basin? In this study, the middle and upper reaches of the Taohe River Basin were selected as the study area. Based on the in-site observations of the meteorological and hydrological stations along with the output data of future climate change scenarios and the SWAT hydrological model, future regional climate change and its impact on runoff change are comprehensively analyzed. Our study aims to optimize water resource scheduling and to improve water use efficiency, which would promote ecological protection and high-quality development in the Taohe River Basin. Our research results can provide a scientific reference for regional long-term water resource management in the arid and semi-arid regions of northwest China.

2. Study Area

The Taohe River (101°36′–104°20′ E, 34° 03′–36°01′ N) is located in the arid and semi-arid areas of northwest China, and it is a main tributary in the upper Yellow River. The total length of Taohe River is about 678 km, and its area is about 25,500 km^2. The Taohe River Basin is located in the transition of the Tibetan Plateau and Loess Plateau, which is also a transition area from alpine humid areas to warm arid areas (Figure 1a,b).

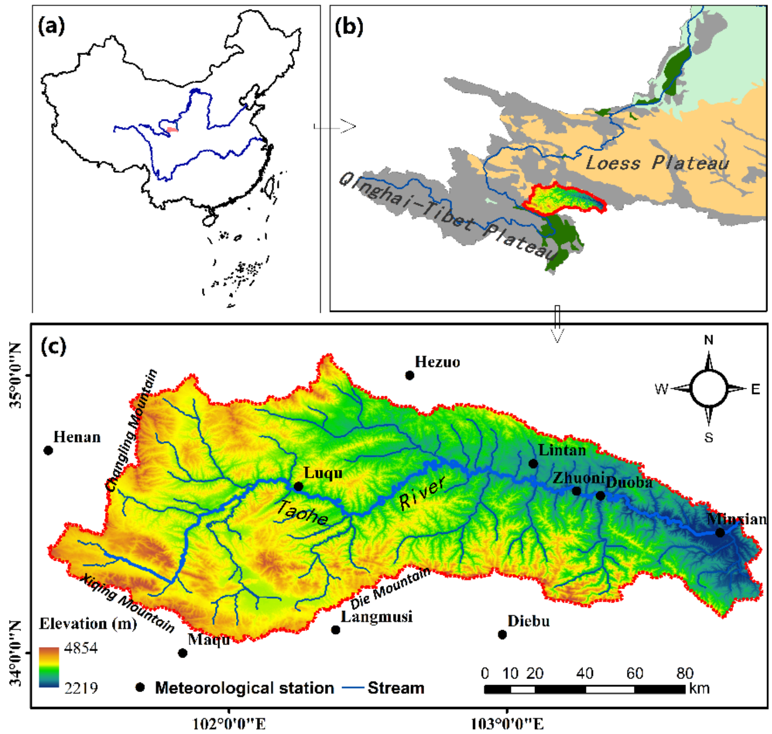

Figure 1. (**a**) Upper Taohe River Basin in China (**b**) Upper Taohe River Basin between Qinghai-Tibet Plateau and Loess Plateau (**c**) Topographical and geomorphic map of upper Taohe River Basin.

The upper Taohe River basin is an important water concentration area in northwest China. It is susceptible to the influence of the southwest monsoon originating from the Indian Ocean, and receives abundant precipitation of 400~600 mm per year. Therefore, the natural runoff gradually occupies more than 68.8% of the whole basin, which is the main runoff generation area and an important water supply area of the Taohe River Basin [31–34]. The water systems in the study area are well developed and have many symmetrical tributaries (Figure 1c). Generally, the middle and upper reaches of the Taohe River are important ecological barriers in the upper reaches of the Yellow River and play an important role in maintaining the water resources and ecological security in the Yellow River Basin.

3. Data and Methods

3.1. Climate Change Scenario Data

The future climate change scenario data used in this paper were derived from the RegCM4.6, which is based on the future climate prediction dataset of the National Tibetan plateau Science Data Center (http://data.tpdc.ac.cn/zh-hans/data/ accessed on 18 March 2022) for northwest China. This dataset is based on four different greenhouse gas emission concentrations (RCP2.6, RCP4.5, RCP6.0, and RCP8.5) determined by the HadGEM2-ES of the regional climate model RegCM4.6, which can simulate and predict the average temperature and precipitation in northwest China from 2007 to 2099 [35]. The future climate change output data set has a spatial resolution of 0.25° × 0.25° and 3 h, daily, and yearly temporal intervals that cover northwest China (Gansu, Ningxia, Qinghai, Xinjiang, and Shaanxi Provinces). This study selected climate variables during the period from 2007 to 2099 under three different emission scenarios (RCP2.6, RCP4.5 and RCP8.5) in the middle and upper reaches of the Taohe River basin/UTB as the forcing data for the SWAT model to project future runoff changes.

3.2. Meteorological and Hydrological Data

Data from eight major meteorological stations in the middle and upper reaches of the Taohe River and its surrounding areas were selected as the input data for the hydrological model. Information on major weather stations is shown in Table 1. The meteorological station data during 1986–2018 were obtained from the China National Meteorological Data Sharing Website (http://data.cma.cn/ accessed on 14 August 2020). The meteorological elements include wind speed, evaporation, atmospheric pressure, temperature (average temperature, maximum temperature, minimum temperature), average vapor pressure, average relative humidity, precipitation, and sunshine hours. The monthly runoff data of the representative hydrological stations (Luqu, Xiabagou, and Minxian) in the middle and upper reaches of the Tao River from 1986 to 2014 were provided by the Gansu Hydrology and Water Resources Bureau (Table 2).

Table 1. Information from main meteorological stations in upper Taohe River Basin.

Station Number	Station Name	Latitude (°)	Longitude (°)	Altitude (m)
56,065	Henan	34.73	101.60	3500.00
56,071	Luqu	34.60	102.50	3191.00
56,074	Maqu	34.00	102.08	3471.00
56,080	Hezuo	35.00	102.90	2910.00
56,081	Lintan	34.70	103.35	2810.00
56,082	Zhuoni	34.58	103.50	2592.00
56,093	Minxian	34.43	104.02	2315.00
52,978	Xiahe	35.18	102.5	2948.00

Table 2. Information of main hydrographic stations in the upper Taohe River Basin.

Station Number	Latitude	Longitude	Catchment Area (km^2)	Data Range (Year)
Luqu	34°35′	102°27′	5043	1986.1~2014.12
Xiabagou	34°41′	103°00′	7311	1986.1~2014.12
Minxian	34°26′	104°02′	14,912	1986.1~2014.12

3.3. SWAT Model Construction Data

The soil and water assessment tool (SWAT) is a well-known hydrological modeling tool that has been applied in various hydrologic simulations. It has been applied to analyze soil water conservation structures and their impacts on reducing runoff. The SWAT model has been demonstrated to be a powerful tool when selecting the most technically effective management strategies to reduce soil degradation [36].

The upper Taohe River Basin can be extracted and divided into 28 subbasins and 388 hydrological response units (HRUs) from DEM. Monthly runoff data from three hydrological stations from 1986 to 2010 are regarded as the calibration period, and data from the period from 2011 to 2014 are used for verification. SWAT-CUP is used for parameter sensitivity analysis and uncertainty analysis.

The land use data used in this research are from the Resource and Environmental Science Data Center of the Chinese Academy of Sciences (http://www.resdc.cn accessed on 10 may 2021). There are some differences between China's land use classification system and the SWAT model, and it is necessary to reclassify regional land use data. After reclassification, there are 6 first-level types and 19 s-level types of land use that can be produced in the upper Taohe River Basin. They are divided into nine new land types (Table 3) to highlight the main land use distribution characteristics of the basin.

Table 3. The reclassification (to SWAT codes) of land use in upper Taohe River Basin.

Number	Type	SAWT Code	Number	Type	SWAT Code
12	Dry land	AGRL	43	Reservoirs, Ponds	WATR
21	Dry land	FRST	46	Beach land	WATR
22	Shrub forest	FRST	51	Towns	URHD
23	Sparse woodland	FRST	52	Rural settlements	URLD
24	Other woodlands	FRST	53	Construction land	UIDU
31	High coverage grassland	PAST	64	Marshland	WETL
32	Medium coverage grassland	PAST	65	Naked land	BARR
33	Low-coverage grassland	PAST	66	Bare rock gravel land	BARR
41	Canal	WATR	67	Other unused land	BARR
42	Lakes	WATR			

Data on the spatial distribution of soil types were derived from the HWSD (China Soil Map-Based Harmonized World Soil Database) Soil Database (http://www.fao.org accessed on 16 October 2021), which was jointly issued by the Food and Agriculture Organization of the United Nations (FAO) and the Vienna International Institute for Applied Systems (IIASA) in 2009. Soil type data (China Soil Map Based Harmonized World Soil Database) from the Nanjing Soil Research Institute, Chinese Academy of Sciences, v1.1 with a 1 km resolution was used to provide reliable soil parameters for SWAT. The SWAT model has collected a large number of physical and mathematical equations to describe the hydrological processes and material transport processes, and many parameters have been applied, most of which have clear hydrological physical significance, main parameters are shown in Table 4.

Table 4. Selected parameters in the preliminary calibration of the SWAT model.

Parameter Name	Type	Physical Meaning	Adjusting Range
r_CN2	.mgt	SCS runoff curve number; related to regional topography and land cover	(−0.2, 0.2)
v_ALPHA_BF	.gw	ALPHA factor (day) indicating the recharge of groundwater and soil water to runoff; directly affects the flood peak and its decline rate	(0,1)
v_CH_N2	.rte	Manning coefficient of main channel that is inversely proportional to confluence velocity	(0,0.3)
v_CH_K2	.rte	The main river diversion coefficient, default 0, indicates the loss of river transportation	(5, 130)
v_GW_DELAY	.gw	Groundwater lag coefficient (day) used to calculate the amount of recharge per day into the groundwater layer and is related to the depth of the horizontal plane and the characteristics of groundwater force	(30, 450)
v_GWQMN	gw.	Invasion depth of shallow aquifer required for reflux	(0, 2)
v_GW_REVAP	.gw	Correlation coefficient of groundwater reevaporation	(0.02, 0.2)
v_REVAPMN	.gw	The depth of shallow aquifer intrusion required for 'reevaporation' occurs, and reevaporation only occurs when the water content of shallow aquifers exceeds the threshold value	(0,57)
r_SOL_K	.sol	Saturated hydraulic conductivity of the soil layer indicating the size of the resulting interflow	(−0.5, 0.5)
r_SOL_AWC	.sol	Available water content in the soil layer indicates soil water storage capacity	(−0.5, 0.5)
v_ESCO	.hru	Compensation coefficient of soil evaporation	(0, 1)
v_EPCO	.hru	Vegetation transpiration compensation coefficient	(0, 1)
v_SURLAG	.bsn	Surface runoff lag coefficient	(0.05, 24)
v_SFTMP	.bsn	Snowfall base temperature	(−5, 5)
v_SMTFP	.bsn	Snowmelt base temperature	(−5, 5)
v_SMFMX	.bsn	Maximum snowmelt coefficient (occurs in summer solstice)	(1, 8)
v_SMFMN	.bsn	Minimum snowmelt coefficient (occurs in winter solstice)	(1, 8)
v_CANMX	.hru	Maximum interception flow of vegetation canopy	(0, 1)
v_TIMP	.bsn	Temperature lag coefficient after icing	(0, 1)
v_TLAPS	.sub	Vertical lapse rate of temperature	(−8, 50)
v_BIOMIX	.mgt	Biomixing efficiency parameters	(0, 1)
v_RCHRG_DP	.gw	The permeability coefficient of underground aquifers indicates the proportion of return irrigation flowing into the deep groundwater layer	(0, 1)
r_SLSUBBSN	.hru	Average slope length	(−0.2, 0.2)

Note: Calibration method: r_ indicates that the existing parameters will be multiplied by 1 (given value), a_ indicates that the given value will be added to the existing parameters, v_ indicates that the existing parameters will be replaced by the given value.

3.4. Evaluation Indicators

The calibration and verification of the SWAT model was carried out using the Nash efficiency coefficient (*NSE*), certainty coefficient R^2, and relative deviation (*RE*) as evaluation indexes to evaluate the simulation results with the measured values. The *NSE* coefficient reflect the fitting degree between the observed and the simulated values. The closer the NSE coefficient is to 1, the better the simulation effect is. If the *NSE* coefficient is greater than 0.5, the simulation of the model is considered successful. R^2 is used to characterize the correlation degree of the variables, which is used to evaluate the consistency of the change trend between the simulated value and the measured value. The calculated value tends to 1, indicating that the simulation effect is better. It is generally considered that $R^2 > 0.6$ can be used as a criterion for evaluating the correlation between simulated and measured runoff values. *Re* represents the relative deviation between the simulated value and the measured value. The more the calculated value tends to 0, the better the effect is. It is generally believed that $Re < 20\%$, and the simulation results can be accepted [37]. The formulas for the evaluation indicators are presented as Equations (1)–(3).

$$NSE = 1 - \frac{\sum_{i=1}^{n} \left(Q_{sim} - Q_{obs}\right)^2}{\sum_{i=1}^{n} \left(Q_{obs} - \overline{Q}_{obs}\right)^2} \tag{1}$$

$$R^2 = \frac{\left(\sum_{i=1}^{n} \left(Q_{obs} - \overline{Q}_{obs}\right)\left(Q_{sim} - \overline{Q}_{sim}\right)\right)^2}{\sum_{i=1}^{n} \left(Q_{obs} - \overline{Q}_{obs}\right)^2 \sum_{i=1}^{n} \left(Q_{sim} - \overline{Q}_{sim}\right)^2} \tag{2}$$

$$Re = \frac{Q_{sim} - Q_{obs}}{Q_{obs}} \times 100\% \tag{3}$$

n represents the length of the simulation time; $\overline{Q}_{obs}$ and $\overline{Q}_{sim}$ represent the average values of the runoff observation and simulation values in the simulation period, respectively; Q_{obs} and Q_{sim} represent the runoff observation and simulation values in the research time, respectively.

4. Result Analysis

4.1. Climate Change Prediction under Different Scenarios

4.1.1. Evaluation and Correction of Climate Model Output

Products from RegCM4.6 driven by HadGEM2-ES have been used to simulate the future climate patterns in northwest China. Pan et al. [35] found that the temperature bias of HadGEM2-ES is generally within ±2.5 °C in the southeast and in the south during the historical period of 1985–2004. This article has evaluated and revised the temperature output values under the RCP4.5 scenario based on the observed meteorological patterns in the upper Tao River Basin based on the historical period of 2007–2018. The deviation between the simulated value and the measured value is exhibited in Figure 2. The deviation between the simulated value and the measured value is small in summer and large in winter. The maximum temperature deviation can reach 7.5 °C, but the temperature variation is consistent with the observed value (Figure 2). According to the relationship between the altitude and temperature in each site, the average observed temperature from 2007 to 2018 is about 0.8 °C. In comparison, the simulated annual average temperature and the observed multiyear average are largely consistent under the different climate change scenarios. Corrections through inverse deductions between the linear equation and the vertical decline rate of the temperature, the average temperature, and the maximum/minimum temperature are adjusted separately. Therefore, the corrected data are more in line with the actual situation of the study area and meet the research needs of future climate change scenarios.

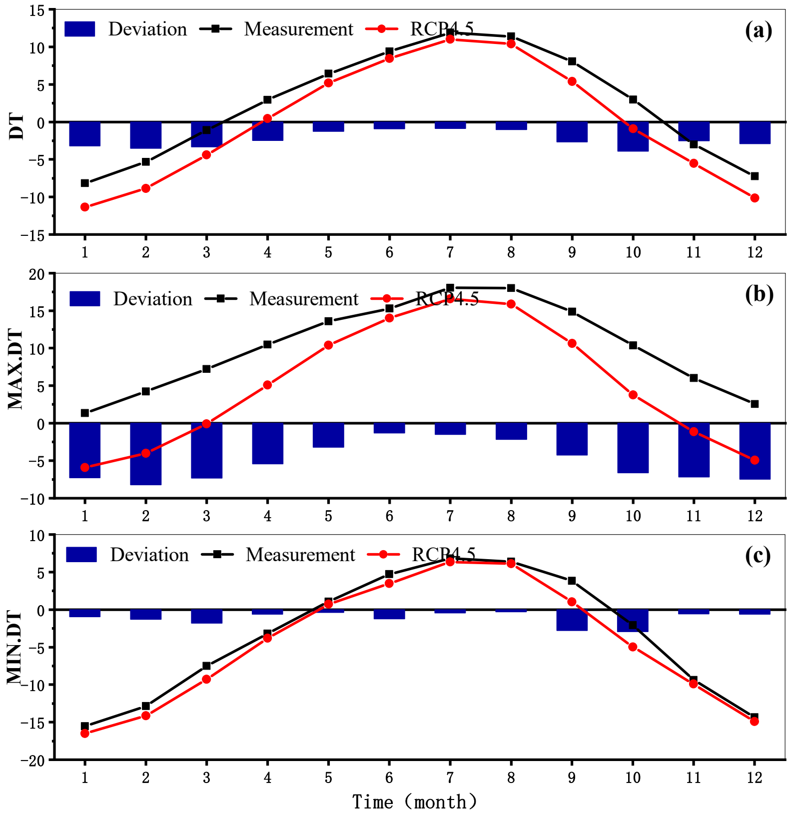

Figure 2. The bias between the observed temperature and simulated temperature in the RCP4.5 scenario in the upper Taohe River Basin. (**a**) Average temperature, (**b**) Maximum temperature, (**c**) Minimum temperature.

4.1.2. Projection of Future Temperature Change in Upper Taohe River Basin

Under the three greenhouse gas emission scenarios, the average annual temperature in the study area shows a consistent warming trend in the future period (Figure 3). The average temperature in the future study area would be about 2.83 °C, 3.32 °C, and 4.24 °C under RCP2.6, RCP4.5, and RCP8.5 during 2007–2100, and the change rates may be 0.10 °C/10a, 0.20 °C/10a, and 0.52 °C/10a. The average temperature in the 2080s would be about 0.54 °C, 1.14 °C, and 3.44 °C higher than the average temperature in 1956–1997 [38], which may be consistent with the global warming trends. Overall, the temperature in the upper Taohe River Basin increases with the increase in emission scenarios.

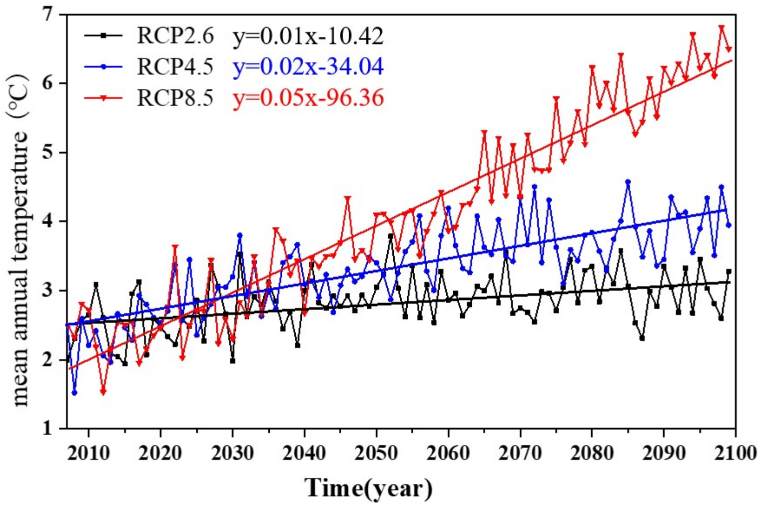

Figure 3. The future changes in temperature at different scenarios in the upper Taohe River Basin.

At the same time, the possible future temperature changes in this basin are also analyzed from the two aspects of maximum and minimum temperatures. The annual average maximum and minimum temperature changes in the upper and middle reaches of the Taohe River under the three greenhouse gas emission scenarios were set for four stages: 2007–2018 and the 2020s (2019–2039), 2050s (2040–2079), and 2080s (2080–2099) (Figure 4).

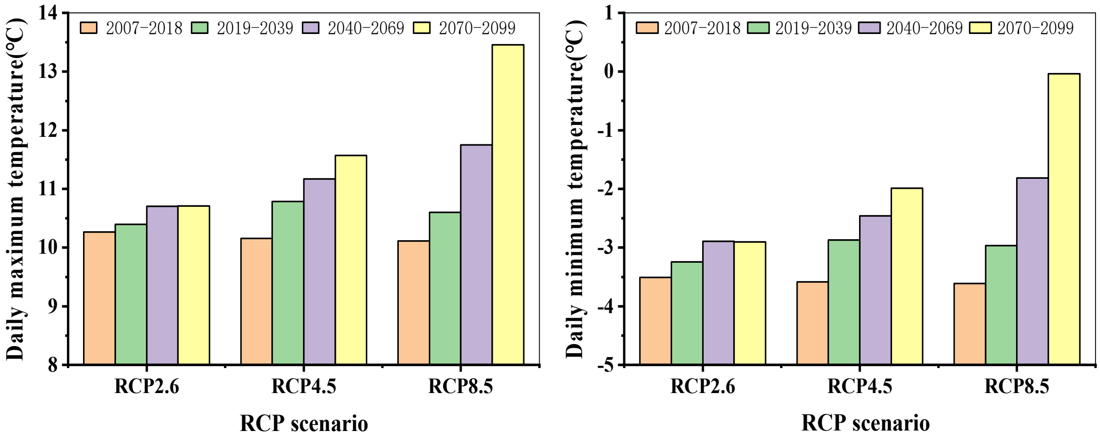

Figure 4. The future changes in the maximum and minimum temperatures under different scenarios.

The maximum temperature and minimum temperature show increasing trends under the three scenarios. The change in the maximum temperature under the RCP2.6 scenario increases steadily, and the increments in the three stages would be 0.13 °C, 0.44 °C, and 0.44 °C higher than those from 2007 to 2018, which is consistent with the change trends in the average temperature. Under the RCP4.5 scenario, the maximum temperature would increase significantly, and the temperature could be 0.63 °C, 1.02 °C, and 1.42 °C higher than in 2007–2018, under the three scenarios, with a maximum change range of 13–17%. The future maximum temperature shows significant changes under the RCP8.5 scenario, which would increase to 0.49 °C, 1.64 °C, and 3.34 °C, which could be higher than the temperature in 2007–2018, with a maximum range of 33%. The results indicate that the highest temperature in the 21st century would increase gradually.

Compared to the maximum temperature variations, the change range of the minimum temperature in different scenarios is consistent with the maximum temperature in the future. Under the RCP2.6 scenario, the minimum temperature in the three stages would increase to 0.26 °C, 0.61 °C, and 0.60 °C, which would be slightly higher than that in 2007–2018, respectively. The change under the RCP4.5 scenario would be significantly enhanced, and the temperatures of the three stages would increase to 0.71 °C, 1.12 °C, and 1.59 °C, which would be higher than those from 2007 to 2018. Under the RCP8.5 scenario, the minimum temperature changed significantly, the minimum temperature would be 0.64 °C, 1.79 °C, and 3.57 °C higher than those from 2007 to 2018. The results indicate that the minimum temperature will increase gradually in the 21st century and that the minimum temperature change would be more significant than the maximum temperature change, which indicates that the minimum temperature changes make an obvious contribution to future regional warming.

4.1.3. Projection of Future Precipitation Change in Upper Taohe River Basin

According to the precipitation data output by the climate model in the historical period (1985~2015) in the northwest region, the simulation effect in the eastern of Qinghai–Tibet Plateau is poor, which may be due to the influence of monsoon circulation on the Qinghai–Tibet Plateau, resulting in a false high-value precipitation center in the climate model. Compared to the observed precipitation from 2007 to 2018 [35], it was found that the simulated precipitation from the climate model is similarly overestimated in the eastern part of the middle and upper reaches of the Taohe River. Therefore, the seriously overestimated stations were removed and compared with the precipitation changes observed by all of the stations in the region. Figure 5 shows the future multiyear precipitation changes in the middle and upper reaches of the Taohe River from 2007 to 2099 and compares the not-removed and removed gridded precipitation. The moving average is a reasonable and practical way to analyze the meteorological data. The 5-year moving average has been selected as a default estimator for the annual survey, partially because it seems easy to understand and compute. The results show that the 5-year moving average curve could be presented as the precipitation change trend.

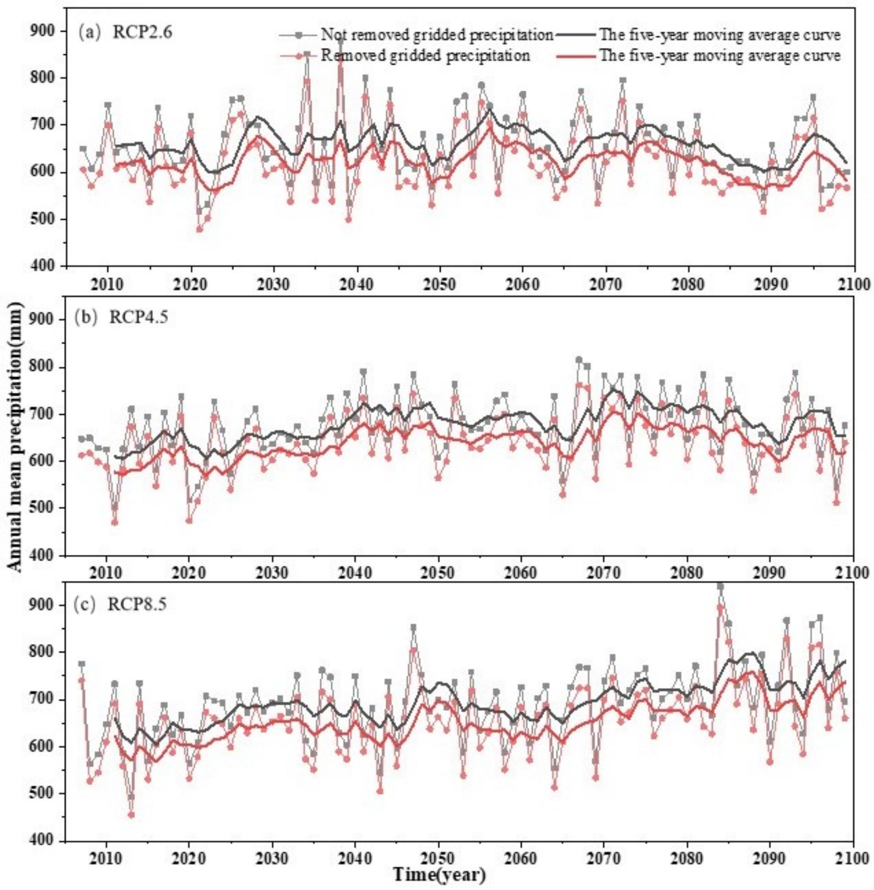

Figure 5. Comparison of future precipitation changes under different climate change scenarios, (**a**) RCP2.6 (**b**) RCP4.5 (**c**) RCP8.5.

Under the RCP2.6 scenario, the average precipitation would be about 658 mm in the study area in 2020–2099, demonstrating an insignificant decreasing trend (−3.69 mm/10a), and the average precipitation after excluding abnormal stations would be 620 mm, which is closer to the measured precipitation. The precipitation would fluctuate greatly in the 2030s, while the precipitation would achieve its lowest level in the 2080s. Under the RCP4.5 scenario, the average precipitation in the future would be 677.5 mm, and the average precipitation after excluding abnormal stations would be 638.5 mm, demonstrating an insignificant increasing trend (4.97 mm/10a). The precipitation would be the highest in the 2070s (689 mm) and would reach its lowest value in the 2020s (591.3 mm). The future average precipitation under the RCP8.5 scenario would reach 693.2 mm, and the average precipitation after excluding abnormal stations would be 653.9 mm, demonstrating an increasing trend (12.28 mm/10a). The average precipitation would experience an insignificant change before the 2080s, but significant fluctuations would appear after the 2080s.

4.2. Applicability Evaluation of SWAT Model

The results of hydrological process curves during the calibration period and verification period showed that SWAT model can capture the time and flow of the flood peaks in the three hydrological stations well (Figure 6). The simulated value in the dry season is also consistent with the basic flow of the basin, but the simulation abilities among the three stations are different. The Luqu, Xiabagou, and Minxian hydrological stations are the main outlets of the source area in the Taohe River. Observational data showed that from 1986 to 2014, the runoff from the Luqu, Xiabagou, and Minxian hydrological stations in the Taohe River Basin showed a significant response to precipitation. From 1986 to 2003, the runoff showed a slight decrease along with precipitation. During 2003 to 2011, the runoff decreased as the precipitation decreased; then, from 2011 to 2014, the runoff increased as the precipitation increased (Figure 6). If we take 1986 to 2010 as the model calibration period and 2011 to 2014 as the model validation period, the SWAT model can capture the variation trends in the three hydrological stations well. The overall runoff simulation values of the determination coefficient R^2, the Nash efficiency coefficient *NSE*, and the relative error *Re* of the monthly runoff simulation at regular rates fall within a small uncertainty interval (Table 5).

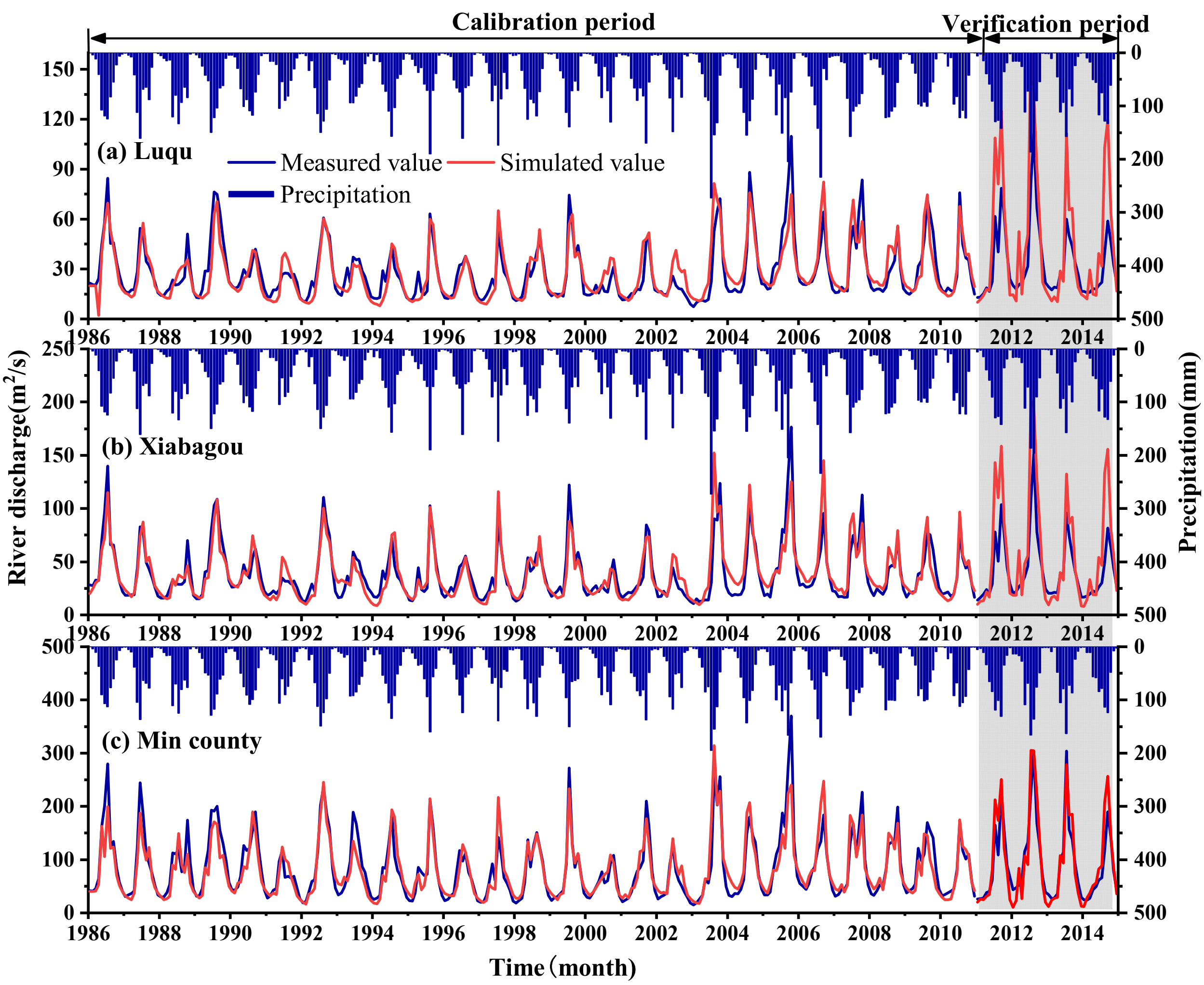

Figure 6. Monthly simulated runoff results during calibration and validation periods in three station, (**a**) Luqu (**b**) Xiabagou (**c**) Min county.

Table 5. Evaluation of runoff simulation results using gage data.

	Period	R^2	*NSE*	*Re*	P-Facor	R-Facor
Luqu	Calibration	0.891	0.793	2.394	0.81	0.75
	Validation	0.952	0.895	−8.991		
Xiabagou	Calibration	0.888	0.779	−3.868	0.93	1.6
	Validation	0.947	0.890	−5.073		
Min county	Calibration	0.914	0.833	−14.615	0.80	0.71
	Validation	0.944	0.875	−8.66		

Luqu station, which is located at the source of the Taohe River Basin, the simulated performance of this station can be easily observed, with R^2, *NSE*, and *Re* showing monthly runoff simulation rates of 0.79, 0.89, and 2.39%, respectively. In the verification period, R^2, *NSE* and *Re* also reached 0.89, 0.95, and −8.9%, respectively. The R^2, *NSE*, and *Re* of the monthly runoff simulation at the Xiabagou station were 0.77, 0.88, and −3.86%, respectively, and 0.89, 0.96, −5.07% during the verification period. The Minxian station serves as the total outlet of the upper Taohe River Basin.

The results showed that monthly runoff simulation rates of R^2, *NSE*, and *Re* were 0.83, 0.91, −14.6%, respectively, and during the verification period, R^2, *NSE*, and *Re* also reached 0.87, 0.94, −8.6%, respectively. The above assessment results indicate that the distributed hydrological model SWAT is feasible to simulate runoff in the middle and upper reaches of Taohe River, which lays a foundation for the subsequent study, which is focus on the response of water resources to climate change in the Taohe River Basin.

The calibration and validation results of three on-site observations showed that the SWAT hydrological model is able to produce an acceptable simulation of runoff at a monthly time step, producing reliable results and meeting the research requirements.

4.3. Projection of Future Runoff Change in the Middle and Upper Reaches of the Tao River

Based on the good application of the SWAT model, the annual runoff changes under the three greenhouse gas emission scenarios in the middle and upper reaches of the Taohe River could be predicted from 2020 to 2099 by inputting the corrected RCP temperatures and eliminating abnormal precipitation data from the grids. As shown in Figure 7, to compare the long-term runoff changes, this research takes the average runoff trends from 1956 to 2014 as the historical period, allowing the runoff changes in different future periods to be analyzed intuitively.

Under the RCP2.6 scenario, the annual average runoff would be about 30.9×10^8 m^3, and the overall change trend is similar to the runoff from 2003 to 2014. Over the whole period, the relative maximum and minimum runoff would alternately appear in the 1930s, while the overall minimum runoff would appear in the mid-1980s and would be as low as 17.1×10^8 m^3. Comparably, the overall average runoff would be the highest in the 1950s, with an annual average runoff of 35.2×10^8 m^3, and would be the lowest in the 1980s at 24.6×10^8 m^3. Drought risk might be estimated in the future. Under the RCP4.5 scenario, the annual average runoff would be about 32.5×10^8 m^3, and the overall change trend is 15% lower than during the period of 1956−1985. The highest runoff values might be observed during the 2040s and 2070s. Under the RCP8.5 scenario, the annual average runoff would be about 32.2×10^8 m^3, with no significant increasing trend being observed. The maximum runoff would appear in the mid-2080s, and the minimum would appear in the mid-2060s and would be as low as 14.8×10^8 m^3.

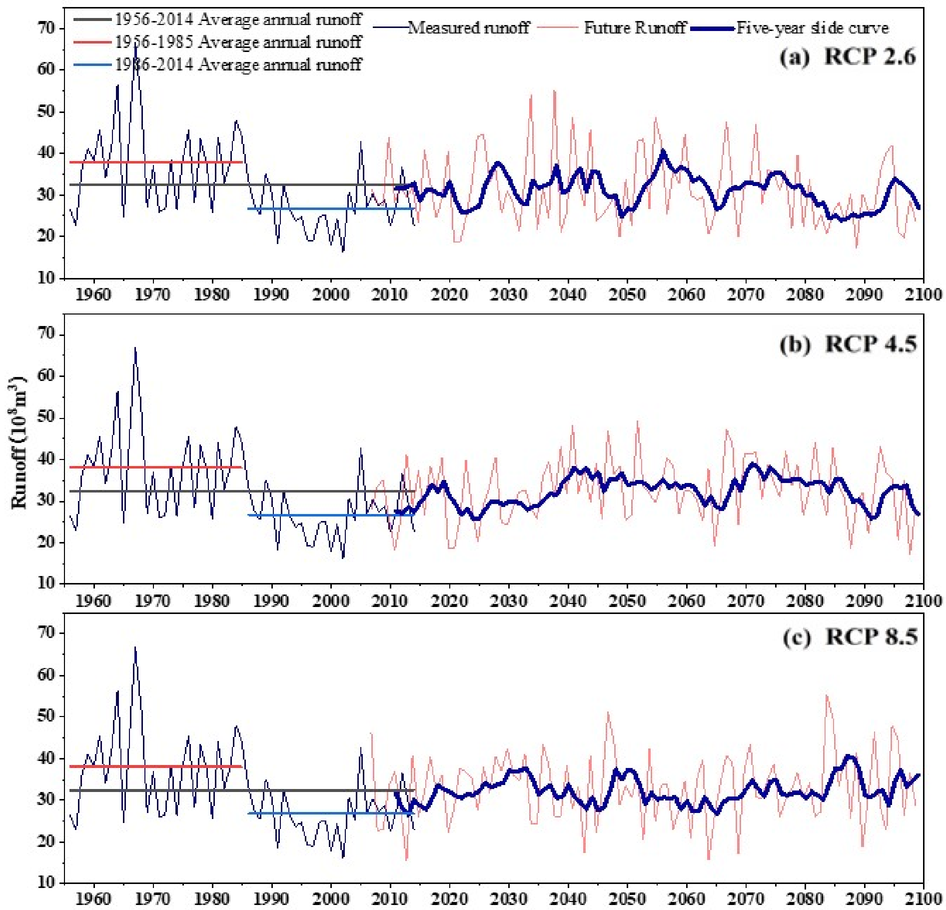

Figure 7. The future changes in runoff at different scenarios in the upper Taohe River Basin, (**a**) RCP2.6 (**b**) RCP4.5 (**c**) RCP8.5.

Table 6 shows the projected runoff changes in each season. Under the RCP2.6 scenario, runoff would decrease significantly in summer, and insignificant changes would be observed during the other seasons. Under the RCP4.5 and RCP8.5 scenarios, the runoff in all seasons would show a fluctuating trend. In general, the future runoff in the upper Taohe River Basin would show a decreasing trend in summer and increasing in autumn. In other seasons, significant fluctuations can be observed the future runoff.

Table 6. The seasonal changes in runoff under different scenarios (unit: 10^8 m^3).

	Time Period	Spring	Summer	Autumn	Winter
RCP2.6	2020~2039	3.43	15.05	11.69	1.61
	2040~2069	3.42	14.78	12.33	1.66
	2070~2099	3.22	12.69	11.63	1.60
RCP4.5	2020~2039	2.65	14.19	11.17	1.48
	2040~2069	3.18	15.07	13.46	1.95
	2070~2099	3.02	14.58	13.27	1.78
RCP8.5	2020~2039	3.81	15.82	11.88	1.37
	2040~2069	3.09	13.56	12.28	1.89
	2070~2099	3.29	14.72	13.99	1.81

5. Discussion

5.1. Uncertainty Analysis of SWAT Model

The SWAT model has a complex structure and involves many equations and variables [39]. Due to the complexity and randomness of hydrological processes, there are many uncertain factors in the processes of hydrological model simulation that could cause interference to the simulation effect. According to the observed situation in the upper Taohe River Basin and in the relevant literature, 23 parameters in the SWAT model were selected for the preliminary overall sensitivity analysis. The calibration number was set to 500 times, and the iteration number was set to 10 times. The parameters suitable for the hydrological process changes in the study area were selected carefully and thoroughly. The contribution of different parameters to the calibration and validation of the model in different study areas are also different and can have a varying degree of impact on the model results [40,41].

5.2. Uncertainty Analysis of Future Climate Change Scenarios

In this study, RegCM4.6 driven by the global climate model HadGEM2-ES was used to simulate future climate change in northwest China. Pan et al. [35] compared the historical period (198–2014) and found that the output results of the model had relatively large simulation errors in the middle and upper reaches of the Taohe River, regardless of the average temperature or precipitation. Because the Taohe River is located at the junction of the Tibetan Plateau and the Loess Plateau, it is jointly affected by the southwest monsoon and the East Asian monsoon as well as by the climate fluctuations of the Tibetan Plateau, and the atmospheric circulation changes are also complex. Together with the rugged terrain and inhomogeneous underlying surface characteristics, it is difficult to obtain accurate model simulations [42]. Moreover, the meteorological stations in the upper and middle reaches of the Taohe River and its surrounding areas are relatively scarce, and the measured data are limited, greatly affecting the reliability of the simulated values. Under the RCP4.5 scenario, the precipitation in the middle and upper reaches of the Taohe River showed a significant decreasing trend from the late 2070s to the late 2080s, with a change rate of -8.97 mm/10a; under RCP8.5, the precipitation showed a significant upward trend, with a change rate of 6.50 mm/10a during the same period. This uncertainty stems from the differences in the scenarios, which will increase the uncertainty of future precipitation trends.

Future climate prediction is complex and highly uncertain, increasing the uncertainty in the exploration of the impact of climate change on watershed hydrological processes. There are many sources of uncertainty in climate prediction, including different future greenhouse gas emission scenarios, natural variability within the climate system, and climate process description methods [43,44]. Even though scenarios and models cannot completely overcome these uncertainties, to deepen the understanding of various physical processes in the climate system, the output results of climate models will become increasingly accurate.

6. Research Limitation and Implication

We have deployed instruments in regions (such as the Qilian Mountains) containing the cryosphere, and the time series of observation data are too short to support a complete watershed runoff simulation. It needs to be emphasized that the study area selected in this article is in a semi-arid area, where the distribution of cryosphere elements is negligible and their impact on runoff can be basically ignored, so runoff in this area is mainly affected by climate (temperature and precipitation). In the future, it is necessary to select areas covered by cryospheric elements for further comparative analysis to separate the contributions of cryospheric elements and climate on watershed runoff.

The precipitation results of other models have some common results and some non-common ones, but the precipitation results of the RCMs are quite heterogeneous. Different simulation ranges, physical parameterization schemes, dynamic frameworks, and atmospheric boundary condition data will have a greater impact on precipitation [19]. Conditional data will have a greater impact on precipitation. This paper is an attempt to use the simulation results of RCM to drive SWAT for runoff simulation, deepening our understanding of climate change impact on runoff changes in the Taohe River basin. In the future, multiple RCMs need to be used for comprehensive evaluation to provide more reasonable runoff simulation results.

7. Conclusions

In this paper, based on the on-site observations of meteorological and hydrological stations along with the output data from future climate change scenarios and the SWAT hydrological model, future regional climate change and its impact on runoff changes were comprehensively analyzed, and the following conclusions were obtained:

Due to the differences in the emission scenarios, the warming amplitude is different. From 2020 to 2099, the average temperature change rates under the RCP2.6, RCP4.5, and RCP8.5 scenarios were 0.10 °C/10a, 0.20 °C/10a, and 0.54 °C/10a, respectively. In the RCP2.6 emission scenario, the average precipitation shows a decreasing trend in the future, with a reduction rate of 3.69 mm/10a. Under the RCP4.5 and RCP8.5 scenarios, the future precipitation shows an increasing trend, with increasing rates of 4.97 mm/10a and 12.28 mm/10a, respectively.

The calibration and validation results of the three on-site observations (Luqu, Xiabagou, and Minxian) in the upper Taohe River Basin showed that the SWAT hydrological model is able to produce an acceptable runoff simulation at a monthly time step. The R^2 values of the calibration period and the verification period in the Minxian station are 0.91 and 0.94, respectively. The *NSE* values 0.83 and 0.87, representing a reliable result.

In the future, under different climate scenarios, runoff will exhibit droughts and flood disasters. Under the RCP2.6 scenario, the average annual runoff in the upper Taohe River Basin reached about 30.9×10^8 m^3, with significant increasing and decreasing fluctuations. Under the RCP4.5 scenario, the average annual runoff reached 32.5×10^8 m^3, experiencing regular periodic increasing and decreasing changes. Under the RCP8.5 scenario, the average annual runoff in the future would be about 32.2×10^8 m^3. The research results can provide a scientific basis for the efficient management and rational utilization of water resources in the Taohe River Basin.

Author Contributions: Conceptualization, M.Y.; methodology, L.C.; data curation, G.W.; writing—original draft preparation, L.C.; writing—review and editing, L.C. and X.W.; visualization, Y.L.; funding acquisition, M.Y. and X.W. All authors have read and agreed to the published version of the manuscript.

Funding: This work was supported by the National Natural Science Foundation of China (U21A2006 and 41771068), the Strategic Priority Research Program of the Chinese Academy of Sciences (CAS) (XDA20100102), the Second Tibetan Plateau Scientific Expedition and Research Program (STEP) (2019QZKK0208) and the Start-up Funds for Introduced Talent at Lanzhou University (561120217).

Institutional Review Board Statement: Not applicable.

Informed Consent Statement: Not applicable.

Data Availability Statement: The data in this study is confidential. Please contact the corresponding author if necessary.

Conflicts of Interest: The authors declare no conflict of interest.

References

1. Bahrami, E.; Salarijazi, M.; Mohammadrezapour, O.; Jou, P.H. Evaluation of SCS model for flood characteristic prediction in an ungauged catchment considering effects of excess rainfall and base flow separation. *J. Earth Syst. Sci.* **2022**, *131*, 11. [CrossRef]
2. Kousali, M.; Salarijazi, M.; Ghorbani, K. Estimation of non-stationary behavior in annual and seasonal surface freshwater volume discharged into the Gorgan Bay, Iran. *Nat. Resour. Res.* **2022**, *31*, 835–847. [CrossRef]
3. Wang, H.; Qiu, Y.; Jia, Y. Development course and tendency of water resources assessment. *J. Beijing Norm. Univ. (Nat. Sci.)* **2010**, *46*, 274–277.
4. Liu, C.; Li, D.; Tian, Y.; Hao, F.; Yang, G. An application study of DEM based distributed hydrological model on macroscale watershed. *Prog. Geogr.* **2003**, *22*, 437–445.

5. Muhammad, S.; Li, J.; Steiner, J.F.; Shrestha, F.; Shah, G.M.; Berthier, E.; Guo, L.; Wu, L.X.; Tian, L. A holistic view of Shisper Glacier surge and outburst floods: From physical processes to downstream impacts. *Geomat. Nat. Hazards Risk* **2021**, *12*, 2755–2775. [CrossRef]
6. Song, H.S.; Chung, E.S.; Shiru, M.S. Uncertainty analysis of monthly precipitation in gcms using multiple bias correction methods under different RCPs. *Sustainability* **2020**, *12*, 7508. [CrossRef]
7. Mo, X.G.; Hu, S.; Lin, Z.H.; Liu, S.X.; Xia, J. Impacts of climate change on agricultural water resources and adaptation on the North China Plain. *Adv. Clim. Chang. Res.* **2017**, *8*, 93–98. [CrossRef]
8. Ge, Q.S.; Wang, F.; Wang, S.W.; Cheng, B.B. Certainty and Uncertainty in Global Warming Studies. *China Popul. Resour. Environ.* **2014**, *24*, 1–8.
9. Aich, V.; Liersch, S.; Vetter, T.; Fournet, S.; Andersson, J.C.M.; Calmanti, S.; van Weert, F.H.A.; Hattermann, F.F.; Paton, E.N. Flood projections within the niger river basin under future land use and climate change. *Sci. Total Environ.* **2016**, *562*, 666–677. [CrossRef]
10. Lindner, M.; Maroschek, M.; Netherer, S.; Kremer, A.; Barbati, A.; Garcia-Gonzalo, J.; Seidl, R.; Delzon, S.; Corona, P.; Kolström, M.; et al. Climate change impacts, adaptive capacity, and vulnerability of European forest ecosystems. *For. Ecol. Manag.* **2010**, *259*, 698–709. [CrossRef]
11. Piao, S.; Ciais, P.; Huang, Y.; Shen, Z.; Peng, S.; Li, J.; Zhou, L.; Liu, H.; Ma, Y.; Ding, Y.; et al. The impacts of climate change on water resources and agriculture in China. *Nature* **2010**, *467*, 43–51. [CrossRef] [PubMed]
12. Bahrami, E.; Salarijazi, M.; Nejatian, S. Estimation of flood hydrographs in the ungauged mountainous watershed with Gray synthetic unit hydrograph model. *Arab. J. Geosci.* **2022**, *15*, 761. [CrossRef]
13. Gupta, H.V.; Kling, H.; Yilmaz, K.K.; Martinez, G.F. Decomposition of the mean squared error and NSE performance criteria: Implications for improving hydrological modelling. *J. Hydrol.* **2009**, *377*, 80–91. [CrossRef]
14. Moss, R.; Babiker, W.; Brinkman, S.; Calvo, E.; Carter, t.; Edmonds, J.; Elgizouli, I.; Emori, S. Towards New Scenarios for the Analysis of Emissions: Climate Change, Impacts and Response Strategies. *Environ. Policy Collect.* **2008**, *5*, 399–406.
15. IPCC. The physical science basis. In *Contribution of Working Group I to the Fifth Assessment Report of the Intergovernmental Panel on Climate Change*; Cambridge University Press: Cambridge, UK, 2013.
16. Kawase, H.; Nagashima, T.; Sudo, K.; Nozawa, T. Future changes in tropospheric ozone under Representative Concentration Pathways (RCPs). *Geophys. Res. Lett.* **2011**, *38*, L05801. [CrossRef]
17. Kim, S.; Kim, B.; Jun, H.; Kim, H. The Evaluation of Climate Change Impacts on the Water Scarcity of the Han River Basin in South Korea Using High Resolution RCM Data. *J. Korea Water Resour. Assoc.* **2010**, *43*, 295–308. [CrossRef]
18. Giorgi, F.; Brodeur, C.; Bates, G. Regional climate change scenarios over the United States produced with a nested regional climate model. *J. Clim.* **1994**, *7*, 375–399. [CrossRef]
19. Wang, X.; Chen, D.; Pang, G.; Gou, X.; Yang, M. Historical and future climates over the upper and middle reaches of the Yellow River Basin simulated by a regional climate model in CORDEX. *Clim. Dyn.* **2021**, *56*, 2749–2771. [CrossRef]
20. Latif, Y.; Ma, Y.; Ma, W.; Muhammad, S.; Muhammad, Y. Snowmelt Runoff Simulation During Early 21st Century Using Hydrological Modelling in the Snow-Fed Terrain of Gilgit River Basin (Pakistan). In *Advances in Sustainable and Environmental Hydrology, Hydrogeology, Hydrochemistry and Water Resource*; Chaminé, H.I., Barbieri, M., Kisi, O., Chen, M., Merkel, B.J., Eds.; Advances in Science, Technology & Innovation; Springer International Publishing: Cham, Switzerland, 2019. [CrossRef]
21. Latif, Y.; Ma, Y.; Ma, W.; Muhammad, S. Differentiating Snow and Glacier Melt Contribution to Runoff in the Gilgit River Basin via Degree-Day Modelling Approach. *Atmosphere* **2020**, *11*, 1023. [CrossRef]
22. Arnold, J.G.; Moriasi, D.N.; Gassman, P.W.; Abbaspour, K.C.; Jha, M.K. SWAT: Model Use, Calibration, and Validation. *Trans. ASABE* **2012**, *55*, 1345–1352. [CrossRef]
23. Srinivasan, R.; Arnold, J.G.; Jones, C.A. Hydrologic Modelling of the United States with the Soil and Water Assessment Tool. *Int. J. Water Resour. Dev.* **1998**, *14*, 315–325. [CrossRef]
24. Zhang, Y.; You, Q.; Chen, C.; Ge, J. Impacts of climate change on stream flows under RCP scenarios: A case study in Xin River Basin, China. *Atmos. Res.* **2016**, *178*, 521–534. [CrossRef]
25. Zhou, J.; He, D.; Xie, Y.; Liu, Y.; Yang, Y.; Sheng, H.; Guo, H.; Zhao, L.; Zou, R. Integrated SWAT model and statistical downscaling for estimating streamflow response to climate change in the Lake Dianchi watershed, China. *Stoch. Environ. Res. Risk Assess.* **2015**, *29*, 1193–1210. [CrossRef]
26. Gao, G.; Zeng, X.; Su, B.; Wen, Y.; Jin, Z.; Wu, B. Proiected Stream Flow in the Huaihe River in 2010–2100. *Adv. Clim. Change Res.* **2010**, *6*, 15–21.
27. Wang, H.; Sun, F.; Xia, J.; Liu, W. Impact of LUCC on streamflow based on the SWAT model over the Wei River basin on the Loess Plateau in China. *Hydrol. Earth Syst. Sci.* **2017**, *21*, 1929–1945. [CrossRef]
28. Zubaida, M.; Shi, Q.; Polat, M.; Zhang, R. Land use and climate change effects on runoff in the upper Urumqi River watershed: A SWAT model-based analysis. *Acta Ecol. Sin.* **2018**, *38*, 5149–5157.
29. Wang, S.; Liu, X. Runoff Response of Zamu River Basin to IPCC Climate Change Scenarios in Northwest China. *Commun. Comput. Inf. Sci.* **2013**, *399*, 223–231.
30. Jin, J.; Wang, G.; Liu, C.; Bao, Z. Future Evolution Trends of Water Resources in Haihe River Basin under the Climate Change. *J. North China Univ. Water Resour. Electr. Power* **2016**, *37*, 1.

31. Cheng, L.; Yang, M.; Wang, X.; Wan, G. Spatial and Temporal Variations of Terrestrial Evapotranspiration in the Upper Taohe River Basin from 2001 to 2018 Based on MOD16 ET Data. *Adv. Meteorol.* **2020**, *2020*, 3721414. [CrossRef]
32. Qi, G.; Zhang, K. Effectiveness and Problems of Forest Protection and Utilization in Qiaohe Forest Region. *China Agric. Inf.* **2015**, *11*, 69–76.
33. Zhang, H. *Water Resources Optimal Operation and Allocation in the Taohe River Basin*; Xi'an University of Technology: Xi'an, China, 2006.
34. Ma, L. Analysis on Hydrological Characteristics of Minxian Hydrological Station in Taohe River. *Gansu Water Conserv. Hydropower Technol.* **2009**, *45*, 9–13.
35. Pan, X.; Zhang, L.; Huang, C. Future Climate Projection in Northwest China with RegCM4.6. *Earth Space Sci.* **2020**, *7*, e2019EA000819. [CrossRef]
36. Akoko, G.; Tu, H.L.; Gomi, T.; Kato, T. A Review of SWAT Model Application in Africa. *Water* **2021**, *13*, 1313. [CrossRef]
37. Xiao, J. *Non-Point Source Pollution Model: SWAT User Application Guide*; Geological Publishing House: Beijing, China, 2010.
38. Cheng, L.; Ma, L.; Yang, M.; Wan, G.; Wang, X. Changes of temperature and precipitation and their impacts on runoff in the upper Taohe River in northwest China from 1956 to 2014. *Environ. Earth Sci.* **2019**, *78*, 423. [CrossRef]
39. Wang, Z.; Liu, C.; Huang, Y. The Theory of SWAT Model and its Application in Heihe Basin. *Prog. Geogr.* **2003**, *22*, 79–86.
40. Rui, X.; Zhu, Q. Some Problems in Research of Distributed Watershed Hydrological Model. *Adv. Sci. Technol. Water Resour.* **2002**, *22*, 56–58.
41. Yang, J.; Gao, X.; Li, Q.; Chen, Q.; Feng, S. SWAT Model Construction and Parameter Uncertainty Analysis in Huangshui Basin. *Res. Soil Water Conscrvation* **2013**, *20*, 82–88.
42. Wang, H.; Wu, Y.; Cui, Y. Evaluating the progress of the CMIP and Its Application Prospect in China. *Adv. Earth Sci.* **2009**, *24*, 461–468.
43. Duan, Q.; Xia, J.; Miao, C.; Sun, Q. The uncertainty in climate change projections by global climate models. *Chin. J. Nat.* **2016**, *38*, 182–188.
44. New, M.G.; Hulme, M. Representing uncertainty in climate change scenarios: A Monte-Carlo approach. *Integr. Assess.* **2000**, *1*, 203–213. [CrossRef]